Structural and Dynamic Properties of Concentrated Alkali Halide Solutions: A Molecular Dynamics Simulation Study

Hao Du,[†] Jayendran C. Rasaiah,[‡] and Jan D. Miller*,[†]

Department of Metallurgical Engineering, 135 South 1460 East, 412 William C. Browning Building, University of Utah, Salt Lake City, Utah 84112, and Department of Chemistry, University of Maine, Orono, Maine 04469

Received: July 22, 2006; In Final Form: November 1, 2006

The physicochemical properties of alkali halide solutions have long been attributed to the collective interactions between ions and water molecules in the solution, yet the structure of water in these systems and its effect on the equilibrium and dynamic properties of these systems are not clearly understood. Here, we present a systematic view of water structure in concentrated alkali halide solutions using molecular dynamics simulations. The results of the simulations show that the size of univalent ions in the solution has a significant effect on the dynamics of ions and other transport properties such as the viscosity that are correlated with the structural properties of water in aqueous ionic solution. Small cations (e.g., Li^+) form electrostatically stabilized hydrophilic hydration shells that are different from the hydration shells of large ions (e.g., Cs^+) which behave more like neutral hydrophobic particles, encapsulated by hydrogen-bonded hydration cages. The properties of solutions with different types of ion solvation change in different ways as the ion concentration increases. Examples of this are the diffusion coefficients of the ions and the viscosities of solutions. In this paper we use molecular dynamics (MD) simulations to study the changes in the equilibrium and transport properties of LiCl, RbCl, and CsI solutions at concentrations from 0.22 to 3.97 M.

I. Introduction

For many years physicochemical properties, such as viscosity, diffusivity, and solubility of brine solutions, have been studied experimentally and theoretically as a function of concentration. The explanation for the dependence of these properties on concentration has been related to the effect of ions on water structure and its dependence on the concentrations of salt solutions. The distinctive feature of water is due to the hydrogen bonding between water molecules, and it is believed that ions of different sizes and charges alter the network structure of water in quite different ways.

Previous viscosity measurements, spectroscopic analysis,[1−9] thermodynamic considerations,[10−14] and flotation tests[15] have revealed that ions of small size (Li^+) interact strongly with water molecules, and form hydrophilic hydration shells, while very large ions behave more nearly like uncharged hydrophobic solutes that interact weakly with surrounding water molecules that form a disordered cage encapsulating the ion.[16,17] X-ray diffraction techniques have shown that the water structure is related to the size of ions in the solution.[18−21] Also, neutron scattering experiments have provided precise information regarding the solvation of water molecules around ions, and illustrate that the water structure is dominated by cation−anion interactions.[22−25]

Molecular dynamics (MD) simulation is a fundamental tool that can be used to explore water/water, water/ion, and ion−ion interactions, and to elucidate the influence of salts on the dynamic properties of brine solutions.[26−29] In the past decade, much research has been devoted to the study of water structure, as well as the dynamic and thermodynamic characteristics of electrolyte solutions.[13,17,28,30−41] Also efforts have been made to characterize the energy parameters of various ions.[35,39,42−44] The thermodynamics of solvation of simple ions as a function of their size, charge, and charge inversion have been studied by MD simulation at infinite dilution extensively,[17] and different types of hydration have been identified and discussed in relation to the energy and entropy of solvation. Systematic investigations by MD simulation of concentrated alkali halide solutions with respect to their effect on water structures and the physicochemical properties of the solutions are limited.

In this paper we use MD simulations to study how a few of the equilibrium and transport properties of aqueous ionic solutions change as the ion concentration increases. We focus our attention on aqueous ionic solutions of LiCl, RbCl, and CsI at concentrations ranging from 0.22 to 3.97M. The solvation of these ions at room temperature and infinite dilution, where ion−ion interactions are absent, exemplifies the different types of hydration that can occur in solution.[17] The present investigations also reveal how the hydration of these ions is altered as the salt concentration increases, and provide valuable information for further X-ray diffraction and neutron scattering studies.

II. Simulation Details

For MD simulations we used the DL_POLY_214 program.[45] A simple cubic cell containing 256 particles including water molecules and ions with periodic boundary conditions was used for the simulation. The extended simple point charge (SPC/E) model for water[46] was used. The initial positions of water molecules and ions were distributed randomly in the simulation cell.

* Address correspondence to this author. E-mail: jan.miller@mines.utah.edu.
[†] University of Utah.
[‡] University of Maine.

10.1021/jp064659o CCC: $37.00
Published on Web 12/14/2006

TABLE 1: Potential Parameters for Water/Water, Water/Ion Interactions

ion/water	σ_{io} (Å)	ϵ_{io} (kJ/mol)	charge (q)	ref
Li^+	2.337	0.6700	1	17
Rb^+	3.348	0.5216	1	13, 17
Cs^+	3.526	0.5216	1	37
Cl^-	3.809	0.5216	−1	42
I^-	4.169	0.5216	−1	46
O	3.169	0.6502	−0.8476	46
H	0	0	0.4238	17, 32, 33

TABLE 2: Average Radii of the First Hydration Shell of Selected Particles

	distance, Å		
particle type	this study (0.22 M)	literature	ref
O	3.33	3.3−3.45	17, 32, 33
Li^+	2.78	2.65, 3.1	17, 32, 33
Rb^+	3.75	3.75, 3.9	17, 32, 33
Cs^+	4.035	3.85, 4.2	17, 32, 42
Cl^-	3.98	3.8, 3.85	17, 32
I^-	4.22	4.3	17

The force field adopted in the present study was a combination of the Lennard-Jones and electrostatic interactions expressed as:

$$\phi(r_{ij}) = 4\epsilon_{ij}\left[\left(\frac{\sigma_{ij}}{r_{ij}}\right)^{12} - \left(\frac{\sigma_{ij}}{r_{ij}}\right)^{6}\right] + \frac{q_i q_j}{r_{ij}} \quad (1)$$

where r_{ij} is the distance between particle i and j, σ and ϵ are the size parameter and energy parameter, respectively, and q_i is the charge of the ith atom (or ion). The intermolecular potential parameters are derived from the work of Dang et al. and are listed in Table 1. The potential parameters for unlike site pairs are expressed via the Lorentz−Berthelot mixing rules:

$$\sigma_{ij} = \frac{\sigma_i + \sigma_j}{2} \quad (2)$$

$$\epsilon_{ij} = \sqrt{\epsilon_i \epsilon_j} \quad (3)$$

Each simulation was for a constant number of ions and water, constant pressure, and constant temperature (NPT) assembly with the pressure fixed at 0.1 MPa and the temperature fixed at 300 K by using a Hoover's thermostat and barostat.[47] The Ewald sum was used to account for the electrostatic interactions. The Leapfrog method with a time step of 1 fs was used to integrate the particle motion. A total simulation time of 1 ns (10^6 steps of 1 fs) including a 200 ps equilibration period was performed. The final results were analyzed for a further simulation of 800 ps after the equilibration period.

III. Results and Discussion

In this section, the MD simulation results were analyzed in terms of the structural and dynamic properties separately. The results are discussed according to ion sizes and their interactions with water molecules.

1. Structural Properties. *1.1. Water/Ion Interactions.* The average radii of the primary hydration shell of selected particles (ion or oxygen atom) determined as the distance to the first minimum in the corresponding pair correlation functions in dilute solutions are listed in Table 2. It is obvious that the size of the hydrated Li^+ ion represented by the primary hydration shell radius of 2.775 Å is much smaller than that of water in its coordination shell, which is 3.325 Å. For larger cations such as Rb^+ and Cs^+, the size of the hydration shell increases accordingly, and is larger than that of the pure water cluster. Similarly, owing to their large size, the Cl^- and I^- hydration shells are much larger than that of the pure water cluster. The size of the hydrated ions will significantly influence the structure of the system, as well as the dynamic properties of the system such as particle diffusion coefficients and system viscosity, which will be further discussed in later sections

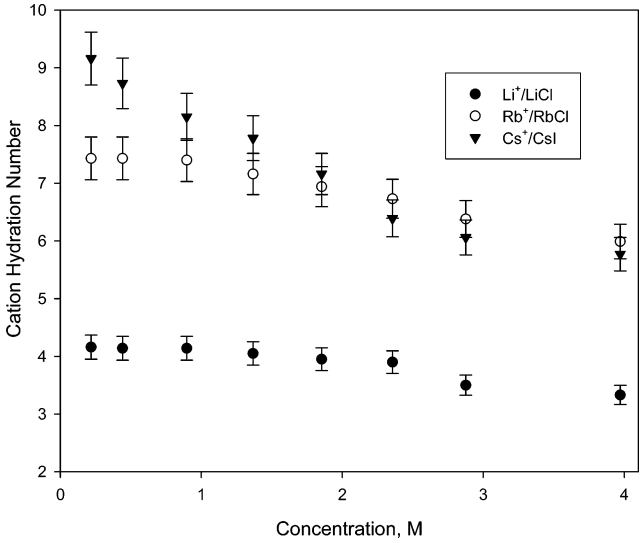

Figure 1. Hydration number of different anions as a function of solution concentration.

The hydration number N_h of ions in the primary shell was calculated from the solute-oxygen radial distribution function (RDF) $g_{io}(r)$ using

$$N_h = 4\pi\rho^* \int_0^{R_1} g_{io}(r) r^2 \, dr \quad (4)$$

where the upper limit corresponds to the first minimum in $g_{io}(r)$ representing the radius for the first hydration sphere, and ρ^* is the density of particles in a given volume.

Figure 1 summarizes the hydration numbers for selected cations as a function of salt concentration. As expected, the hydration number is dependent on ion size, and for the same salt concentration increases as the size increases. As the solution becomes more concentrated, the hydration number of cations decreases monotonically with Cs^+ showing the most significant drop, and Li^+ the smallest decrease. For small ions such as Li^+, the large local electric field binds water molecules in a tetrahedrally coordinated and tightly held hydrophilic hydration shell as shown in Figure 2A. As the solution becomes more concentrated, some of the water molecules participating in the Li^+ ion hydration shell are replaced by negatively charged Cl^- ions as shown in Figure 2B, hence the hydration number of Li^+ ions decreases as the solution concentration increases. The strong hydrophilic hydration effects of Li^+ ions also explain the structure of water around the oppositely charged anions as well as in bulk water in the same solution, which will be discussed in later sections. For very large cations such as a Cs^+ ion, the local electric fields at the ion surface have decreased significantly, and they behave more like uncharged particles.[17] Hence, as the size of the cation increases, the dominating electrostatic hydrophilic hydration of small ions is gradually replaced by hydrophobic hydration of large ions where hydrogen-bonded water molecules form a disordered cage surrounding the ions as can be seen in Figure 3A. When hydrophobic hydration dominates, water molecules are loosely bonded to the ion, and the radius of the primary hydration shell is large,

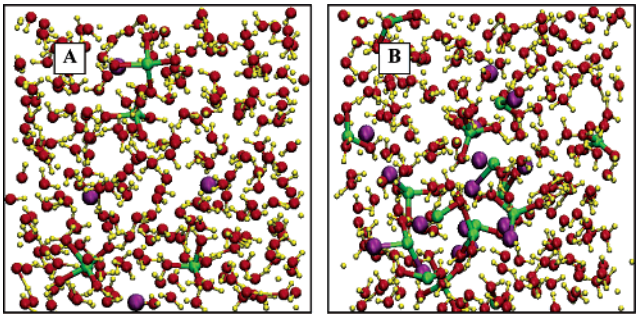

Figure 2. Snapshot from MDS of 0.9 M LiCl solution containing 4 Li^+ and 4 Cl^- (A) and 3.97 M LiCl solution containing 16 Li^+ and 16 Cl^- (B). Red, oxygen atom in water; yellow, hydrogen atom; purple, Cl^-; and green, Li^+. Each Li^+ is tetrahedrally bonded with four water molecules at low concentration as seen in Figure 1A. When the solution becomes concentrated, some water molecules in the Li^+ tetrahedral hydration shell are replaced by Cl^-, forming direct cation/anion pairing as seen in Figure 1B.

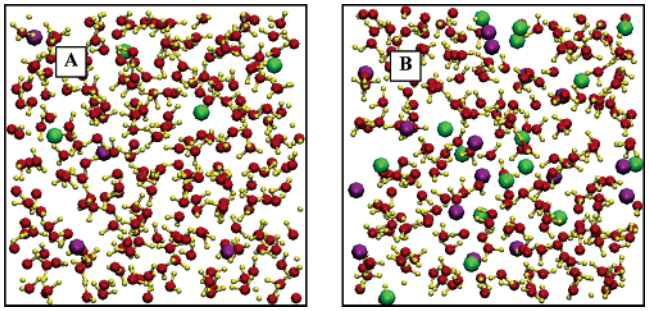

Figure 3. Snapshot from MDS of 0.9 M CsI solution containing 4 Cs^+ and 4 I^- (A) and 3.97 M CsI solution containing 16 Cs^+ and 16 I^- (B). Red, oxygen atom in water; yellow, hydrogen atom; purple, I^-; and green, Cs^+. Water molecules form hydrophobic cages around cations, and stable hydration shells around anions. At high solution concentration, cations and anions pair up minimizing the number of water molecules in the primary hydration shell around ions.

allowing more water molecules to be accommodated. As the number of ions increases in the solution, there will be fewer water molecules available to complete the cages around ions, and the cations and anions will pair up to include fewer water molecules in their hydration shells which are fragile and may break, as observed from Figure 3B. Therefore, the hydration number around these ions decreases with concentration and more dramatically for large ions than it does for the small Li^+ ions. The change of hydration number with salt concentration reveals the balance between the tendency for water molecules to be associated with each other as pure water clusters and the tendency to be associated with ions as hydration shells.

For anions, some interesting results have been observed in our simulations. As seen in Figure 4, in LiCl solutions, the hydration number for Cl^- was found to increase slightly until the salt concentration increased to 3.97 M. But when the cation is Rb^+, the hydration number of Cl^- decreases with respect to concentration. This means that the size of the cation has a substantial influence on the structure of water molecules not only around the cation but also around anions when the concentration is high. First of all, due to the asymmetry of the water molecule, the hydration state of anions is different than that of cations with similar size as shown schematically in Figure 5, and is energetically more favorable. Thus, in this arrangement water molecules can accommodate themselves stably around anions. In LiCl solutions, as seen from Figure 2B, it is clear that, as the salt concentration increases, Cl^- ions will replace some of the water molecules in the Li^+ ion tetrahedral hydration

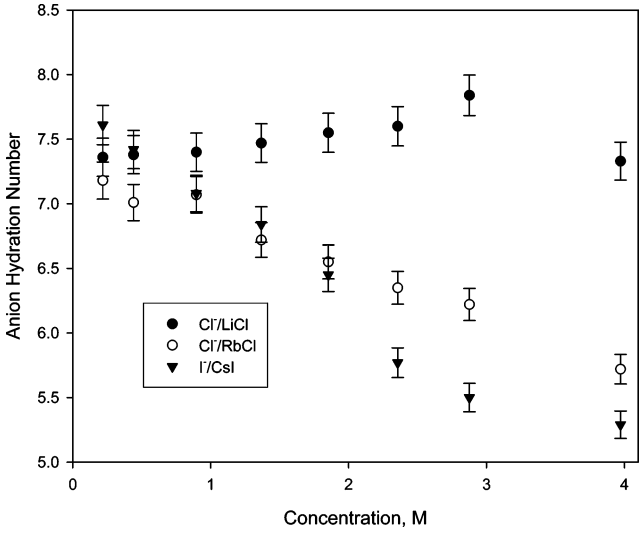

Figure 4. Hydration number of different anions as a function of solution concentration.

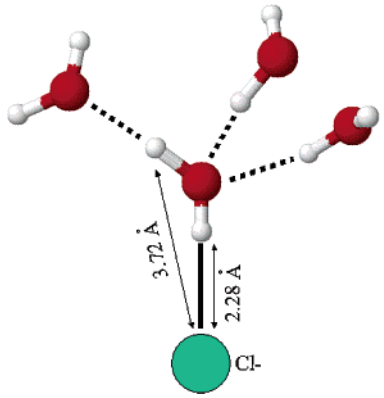

Figure 5. Schematic model showing the hydration of Cl^-. All the distances shown are obtained from $g_{ClO}(r)$. The orientation of the water molecule directly bonded with the Cl^- is due to the asymmetry of water molecules, and thus the hydration of Cl^- is energetically more stable than the hydration of similar sized cations.

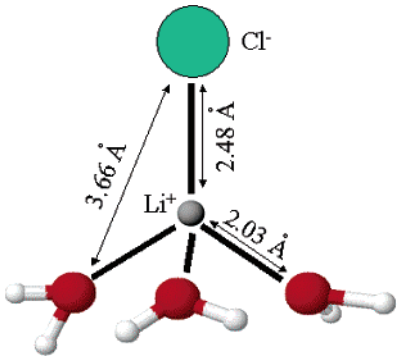

Figure 6. Schematic model showing the replacement of one water molecule in a Li^+ tetrahedral hydration structure with a Cl^-. The three water molecules are within the distance to be included into the primary hydration shell of Cl^-.

structure. When this happens, as shown schematically in Figure 6, the distance between the Cl^- ion and the water molecules in the Li^+ tetrahedral hydration shell is around 3.66 Å, which is very close to the distance of primary minimum in the Cl−O radial distribution function $g_{OCl}(r)$, and therefore, these water molecules are counted into the hydration shell of the Cl^- ion. The more ions in the solution, the greater the possibility for the Cl^- and Li^+ to pair up, leading, therefore, to the larger

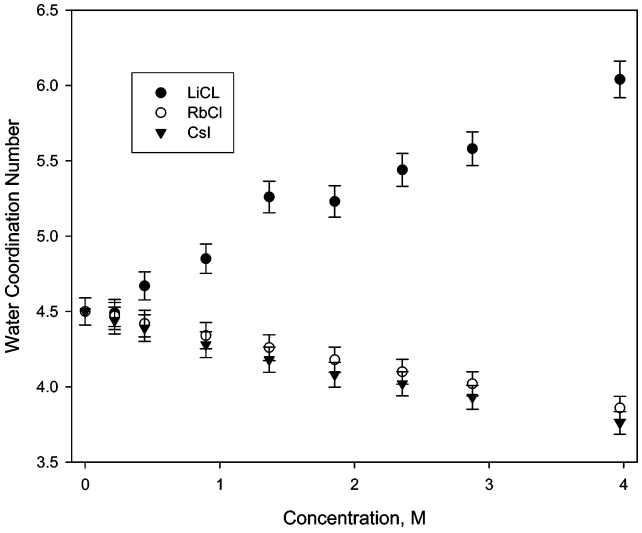

Figure 7. The first shell water/water coordination numbers as a function of solution concentration in different salt solutions.

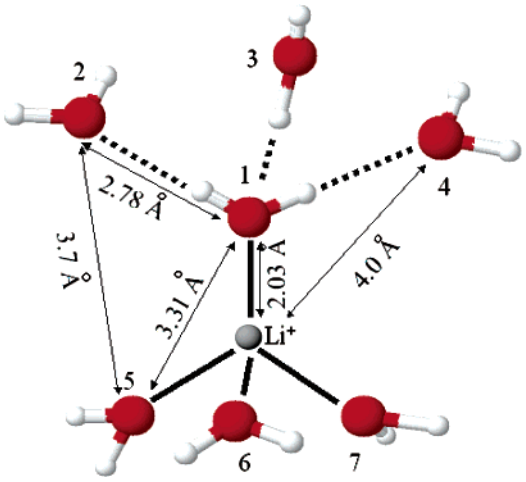

Figure 8. Schematic model showing the hydration of Li^+ with distances between particles obtained from the radial distribution functions. It is shown that water 5, 6, and 7 are within the distance to be included into the primary shell of water 1.

hydration number of the Cl^- ions. At very high solution concentration, as many as three Cl^- ions can directly bond with one Li^+ ion as seen in Figure 2B, therefore fewer water molecules are in the Cl^- hydration shell, thus, the hydration number decreases. The discrepancy of Cl^- ion hydration number at high concentration between neutron scattering experiment (~5.5)[25] and this study (~7.2) is due to the fact that in neutron scattering experiments, the hydration number is calculated based on correlation between the Cl^- ion and deuterium atoms in D_2O ($g_{DCl}(r)$), whereas in this study, the calculation is based on the correlation between the Cl^- ion and the oxygen atom in H_2O ($g_{OCl}(r)$). From Figure 6, it is clear that when $g_{HCl}(r)$ is used to calculate the Cl^- ion hydration number, the distance between the Cl^- ion and the hydrogen atoms is larger than the distance of the primary minimum in the $g_{HCl}(r)$, due to the orientation of the water molecules bonded with the Li^+ ion (water hydrogen atoms pointing away from the Cl^- ion). Therefore, these Li^+ ion bonded water molecules are not counted in the primary Cl^- ion hydration shell in the data from neutron scattering experiments. Further, at 3.97 M, the Cl^- ion hydration number based on $g_{HCl}(r)$ is about 5.66 in this study, which is in very good agreement with neutron scattering study results.[25] For Rb^+, which is a big cation, water molecules form a loose hydration shell as mentioned previously. For the same reason that the hydration number around large cations decreases with solution concentration, the hydration numbers around Cl^- ions in RbCl solutions as well as I^- ions in CsI solutions become smaller in more concentrated solutions.

1.2. Water/Water Interactions. Water molecules are capable of forming hydrogen bonds, and the number of water molecules directly bonded with a reference water molecule is the primary shell water/water coordination number. The variation of the primary shell water/water coordination number with concentration for different brine solutions is summarized in Figure 7.

The variation of water/water coordination is explained in terms of the different hydration structures of ions in the solution. In pure water, water molecules form dynamic tetrahedral networks. When Li^+ ions are present, some water molecules will be tetrahedrally bonded around Li^+ ions. As shown schematically in Figure 8, when calculating the coordination number of water 1, besides water 2, 3, and 4, which are directly hydrogen bonded with water 1, water 5, 6, and 7 will also be counted because the distance between water 1 and water 5, 6, and 7, which is around 3.31 Å, is very close to the distance of the primary minimum of pure water from the radial distribution function $g_{OO}(r)$, which is 3.33 Å. Therefore, the coordination number of water 1 is six. As more Li^+ ions are present, the number of water molecules tetrahedrally bonded with Li^+ ions increases accordingly, and one direct result is the water/water coordination number increases with salt concentration.

Further, at very high solution concentration (3.97 M in this study), the first minimum of the O−O radial distribution function can be as large as 3.7 Å, which is also the theoretically closest distance between water 1 and water molecules that tetrahedrally bonded with water 5, 6, and 7 as is schematically shown in Figure 8. Also, at very high solution concentration, as previously discussed, Cl^- can replace water molecules in the Li^+ ion tetrahedral structure, which leads to the fact that some of the water molecules in the Cl^- ion hydration shell are within the distance to be counted as coordinating with water molecules in the Li^+ ion tetrahedral structure. All these factors contribute to the large water/water coordination number at high solution concentration.

In contrast, when large Cs^+ ions are in the solution, water molecules are loosely caged around these ions. For water molecules composing the cages, because one position has been taken by these large ions, only three other water molecules can be hydrogen bonded to them and counted as primary waters of coordination, thus, the water/water coordination number of these cation bonded water molecules is less than that of the pure water cluster. As more ions are in the solution, more water molecules will be around ions, and consequently, the water/water hydration number decreases monotonically with salt concentrations.

In this study, we did not distinguish the water molecules in pure water clusters and those that participate in ion hydration, which play a significant role in terms of the water/water hydration number when the solution concentration is high. For example, in 3.97 M LiCl solution, there are 16 cations, 16 anions, and 224 water molecules. Around each Li^+ ion, there are about 3.3 tetrahedral bonded water molecules that lead to a total of about 53 water molecules in cation hydration shells. The hydration number of Cl^- is 7.33, which includes the contribution of water molecules bonded to the Li^+ ion that is simultaneously bonded with the Cl^-. Taking this factor into consideration, there are only about 4.2 water molecules directly caged around each Cl^-, totally about 77 water molecules. That leaves 94 water molecules to participate in pure water clusters. The observed large water/water coordination number of 6 at

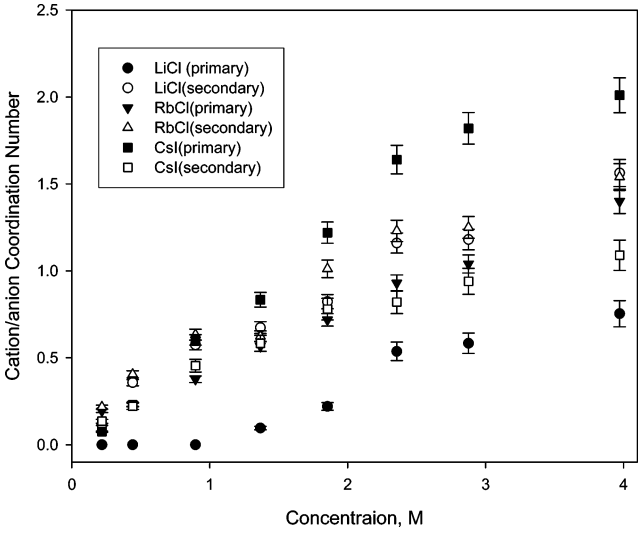

Figure 9. The first and second shell cation/anion coordination number variation as a function of solution concentration for different salts.

this concentration mostly results from the contribution of water molecules around Li^+ ions. Water molecules in the Cl^- hydration shell can also contribute when the Cl^- ion is paired up with Li^+. As to water molecules in pure clusters, their influence is not very significant if any.

1.3. Cation/Anion Interactions. The cation/anion coordination number as a function of salt concentration is summarized in Figure 9 where both the primary and secondary coordination numbers are presented. Generally speaking, independent of ion species, both the primary and secondary coordination numbers between cation and anion increase when the salt concentration increases. Specifically, for the Li^+/Cl^- combination, an increase of the secondary coordination number, which is the interaction of hydrated or solvent separated ions, is much more significant than an increase of the primary coordination number, which is the naked ion−ion interaction. In contrast, for the Cs^+/I^- combination, the primary coordination increases much more significantly with concentration. And for the Rb^+/Cl^- combination, the change in the coordination number for both the primary and the secondary shell is almost of the same magnitude. When Li^+ ions are in the solution, due to the strong local electric fields, water molecules are tightly bonded by Li^+ ions, excluding the direct contact with Cl^- ions. When a large number of ions are in the solution, there is competition between ion/water and ion/ion interactions. Because hydrophilic hydration of Li^+ ions dominates, driven by minimization of system energy, the coordination number between hydrated ions increases more significantly relative to the direct ion/ion contact. For larger ions such as Cs^+ ions, loose hydrophobic hydration shells are formed around these ions. On the other hand, water molecules try to keep their integrity as pure water clusters. Because of the direct cation/anion interaction, which will lead to fewer water molecules participating in the hydration shells (energetically more favorable), the primary coordination number increases faster as a function of salt concentration. For the intermediate ion combination (Rb^+ and Cl^-), the ion/water and the ion/ion interactions are in close competition.

1.4. Further Water Structure Discussion. The ratio R_{iO}, which is expressed as:

$$R_{iO} = \frac{\text{no. of water molecules in the secondary shell of particle i}}{\text{no. of water molecules in the primary shell of particle i}} \quad (5)$$

where the subscript *i* represents the reference particle (ion or water molecule) and the subscript O represents the surrounding water. The variations of R_{iO} as a function of solution concentration are summarized in Table 3 for cation/water, anion/water, and water/water structures, respectively. In pure water, because all the water molecules are dynamically hydrogen bonded with other water molecules, and form tetrahedral structures, the ratio R_{OO} is around 4.5, the same as the primary shell water/water coordination number. For cation hydration shells, it is noticed that there is almost a monotonic increase of R_{LiO} from about 4.0 in very dilute solution to about 4.4 in concentrated solution. At very low concentration, water molecules tetrahedrally bonded with Li^+ ions are also tetrahedrally bonded with other water molecules in bulk. Because the radius of the secondary hydration shell of Li^+ is smaller than the secondary shell for a pure water cluster, fewer water molecules can be accommodated in the secondary hydration shell for Li^+, leading to the observed lower R_{LiO} number when compared to pure water clusters. When the solution concentration is increased, some of the water molecules in the primary Li^+ hydration shell are replaced by Cl^- ions as previously discussed, thus, the number of water molecules in the primary hydration shell of a Li^+ ion is smaller. But some of the water molecules in the Cl^- ion primary hydration shell are included in the secondary hydration shell of the Li^+ ion, therefore, R_{LiO} increases with solution concentration. For larger cations such as Rb^+ and Cs^+, it is obvious that R_{iO} is significantly lower than that of pure water clusters at all solution concentrations. As previously discussed, water molecules loosely bond with large cations. These water molecules participating in ion hydration shells are not able to form a complete tetrahedral water cluster with other water molecules. This breakdown of the continuous water network is most significant in the vicinity of the cations, and leads to the observed decrease of R_{iO}. As the solutions become more concentrated, Rb^+ ions and Cs^+ ions are paired up with corresponding anions in the solutions, and the R_{iO} increases with solution concentration as is the case for Li^+ ions.

TABLE 3: Ratio of Water Molecules in the Secondary Shell to Those in the Primary Shell around Ions (R_{iO}) as a Function of Solution Concentration

	ratio of water molecules in the secondary shell to those in the primary shell around ions (R_{iO})								
concn, M	Li^+	Rb^+	Cs^+	Cl^-/LiCl	Cl^-/RbCl	I^-/CsI	LiCl	RbCl	CsI
0.00	4.51	4.51	4.51	4.51	4.51	4.51	4.51	4.51	4.51
0.22	4.17	2.63	2.21	3.52	3.70	3.72	4.30	4.45	4.43
0.44	4.19	2.65	2.21	3.49	3.79	3.76	4.11	4.38	4.35
0.90	4.22	2.70	2.26	3.41	3.81	3.85	3.87	4.38	4.32
1.37	4.26	2.77	2.38	3.22	3.87	3.85	3.44	4.24	4.27
1.85	4.32	2.82	2.42	3.09	3.85	3.91	3.29	4.23	4.25
2.36	4.38	2.83	2.47	3.08	3.90	3.94	3.03	4.22	4.20
2.88	4.49	2.89	2.63	3.05	3.94	4.00	2.80	4.08	4.16
3.97	4.59	2.89	2.64	2.99	4.12	4.10	2.14	3.93	4.21

TABLE 4: Residence Times of Various Particles as a Function of Solution Concentration

	residence time, ps								
concn, M	Cs^+	Rb^+	Li^+	Cl^-/LiCl	Cl^-/RbCl	I^-/CsI	H_2O/LiCl	H_2O/RbCl	H_2O/CsI
0.22	6.8	7.7	50.4	11	10.4	7.2	5.7	5.6	5.6
0.44	7.4	7.4	54.1	11.3	9.9	7.3	5.7	5.6	5.5
0.9	7.1	8.2	64.1	11.5	10.3	7.3	6.3	5.5	5.5
1.37	6.9	8.1	68.5	12.1	9.8	7.4	6.4	5.4	5.6
1.85	7	7.9	90.1	13.6	10.2	7.1	6.6	5.5	5.4
2.36	7.5	8.7	101	14.3	10.6	7.4	6.9	5.8	5.8
2.88	7.1	8.3	108.7	15.8	10.2	7.5	7.9	5.6	5.4
3.97	7.5	9.1	109.9	16.4	10.6	7.5	7.9	5.6	5.8

For Cl^- ions in LiCl solutions, it is interesting to notice that R_{iO} instead of increasing as a function of solution, decreases. This is because, in LiCl solution, the Cl^- ion can replace water molecules in the primary Li^+ ion hydration shell. Under this condition, all the other water molecules that bonded with the same Li^+ ion will be included in the primary hydration shell of this Cl^- ion, leading to an increased primary hydration number. On the other hand, due to the large distance between Cl^- ion and water molecules in the same primary Li^+ ion hydration shell, water molecules in the secondary hydration shell of this Li^+ ion are not within the distance limit to be included in the secondary hydration shell of the Cl^- ion. Thus, the R_{ClO} in LiCl solution is significantly lower than that of R_{OO} for pure water clusters, and decreases as a function of solution concentration. For Cl^- ions in RbCl solutions and I^- ions in CsI solutions, their R_{iO} variation follows the same trend as that of cations for the same reasons. One issue that needs to be addressed here is that despite the large sizes of these anions, their ability to break tetrahedral water networks is not as significant as that of large cations, as indicated by their larger R_{iO} for the same concentration. This characteristic is explained in terms of the asymmetry of water molecules. Consequently these anions have a greater hydration energy when compared to alkali cations of similar size, and are able to form a more stable hydration shell,[16,17] therefore being less destructive to water structures.

R_{OO} describes the structure of water molecules in the bulk. It can be seen that in LiCl solution, R_{OO} decreases monotonically with the solution concentration for the same reason that explains the changes of R_{ClO} in the same solution. In solutions containing larger cations, water molecules in the bulk maintain their tetrahedral network very well as indicated by the large R_{OO} at all concentrations. The noticeable decrease of R_{OO} in RbCl and CsI solutions with solution concentration is due to the fact that some water molecules participate in the formation of hydration shells around large ions in these solutions. In this way the integrity of tetrahedral water structures is lost. Such an analysis also explains the ion/water and cation/anion structures discussed in the previous sections.

2. Dynamic Properties. *2.1. Residence Times.* The residence time of water in the primary hydration shells of ions, τ , is defined by

$$\tau = \int_0^\infty \langle R(t) \rangle \, dt \tag{6}$$

$\langle R(t) \rangle$ is derived from time correlation functions[17,40,46] and is defined by

$$R(t) = \frac{1}{N_h} \sum_{i=1}^{N_h} [\theta_i(0)\theta_i(t)] \tag{7}$$

where $\theta_i(t)$ is the Heaviside unit step function, which has the value 1 if a water molecule i is in the hydration shell of the ion at time t and zero otherwise. N_h is the hydration number. Following previous work,[17,40,42,48] the residence time can be accurately approximated by numerical integration of $\langle R(t) \rangle$ up to $t = 10$ ps with the remainder calculated by fitting $\langle R(t) \rangle$ at extended time to an exponential decay $e^{-t/\tau'}$. The single time characteristic parameter, τ', would be equal to the actual residence time if the decay of $\langle R(t) \rangle$ was exponential at all times. To take account for the temporary excursion of water molecules in the hydration shell, water molecules absent for less than 2 ps are considered as present. Residence times of various particles as a function of solution concentration using the exponential fit method were calculated and are presented in Table 4 for cations, anions, and water molecules.

First, the residence time for water molecules in the primary water shell increases inversely with ion size for both cations and anions. Small ions such as Li^+ strongly interact with water molecules in the hydration shell and therefore significantly confine the movement of water molecules in the primary water shell, resulting in a substantially longer residence time. For large ions such as Cs^+, Rb^+, and I^-, the local electric fields are weak as discussed earlier, and water molecules in the primary hydration shell are more loosely bonded to them. Thus they are more mobile and the residence time of water is shorter. A similar observation has also been documented in the literature.[17,40] Second, the residence time for water in the primary hydration shell around Li^+ ions increase significantly with solution concentration, while only moderate increase was observed for Rb^+ ions and almost no noticeable change for Cs^+ ions. This can also be explained in terms of different hydration shell structures around these ions. Strong hydrophilic hydration is dominating for small ions. At very high solution concentration, as many as one fourth of the total water molecules are tetrahedrally bonded by Li^+ ions, hence, when one water molecule diffuses away from a Li^+ ion, there is a very good chance for this water molecule to be tetrahedrally bonded by other Li^+ ions, therefore the diffusivity of water molecules around Li^+ ions decreases significantly with solution concentration. This is also the reason for the significantly increased residence times for water molecules around Cl^- ions and within pure water clusters in LiCl solution as a function of solution concentration. When the ion size increases, hydrophobic hydration plays a more significant role and water molecules form cages and bond loosely around ions. Under this condition, the diffusivity of water molecules in pure water clusters and around ions is of the same magnitude. In very concentrated solutions, despite the fact that almost all water molecules participate in the hydration of ions, the mobility of water molecules does not change significantly. Therefore, in CsI solution, the residence time of water does not have a noticeable change with solution concentration. Only a marginal increase was noticed for water molecules in RbCl solutions.

TABLE 5: Comparison of Calculated Diffusion Coefficients at 0.22 M with Values Reported in the Literatures at Infinite Dilution

ion or molecule	diffusion coefficient, 10^{-9} m^2 s^{-1}		
	this study	literature	ref
Li^+	1.06	1.22	17
Rb^+	1.86	1.98	17
Cs^+	1.77	1.88	17, 30, 40
Cl^-	1.6	1.56−1.77	17
I^-	1.59	1.6	46
H_2O	2.5	2.35	17

2.2. Self-Diffusion Coefficients. The tracer diffusion coefficient D_i of an ion can be calculated from its mean square displacement (MSD)[17,40,49] by using the relationship

$$D_i = \lim_{t\to\infty}\frac{1}{6}\langle[r_i(t) - r_i(0)]^2\rangle \quad (8)$$

where $r_i(t)$ is the position of a particle i at time t. The diffusion coefficients of ions in dilute solution (0.22 M in this study) are summarized in Table 5, and compared with literature values at infinite dilution. The diffusion coefficients of ions calculated in the current study are close to the values from the literature, demonstrating that the simulation has been validated. The observed differences in the diffusion coefficients can be explained in terms of the solution concentration in the simulation, which is 0.22 M for the current study and is the infinite dilute state for the references.

The diffusion coefficients for cations, anions, and water are shown as a function of salt concentration in Table 6. From the table, it can be seen that the diffusion coefficients for the ions and water molecules decrease with increasing salt concentration. Close analysis of these data indicates that the decrease in diffusion coefficients with concentration is the smallest for the CsI solution and largest for LiCl solution. In both cases, as the concentration increases, the diffusion coefficients of the cation and anion become more nearly alike. A similar observation has been made in previous studies of aqueous solutions of NaCl and KCl solutions at high concentrations.[40,50] As for the systems containing large ions (Cs^+, Rb^+, and I^-) with weaker electric fields, the observed decrease of ion diffusivity can be explained also in terms of increased ion pairing, which slows down the movement of ions and water molecules bound to them.

The self-diffusion of water molecules in LiCl solution changes dramatically in magnitude as the solution becomes denser. The self-diffusion coefficient of SPC/E water at 25 °C is 2.5×10^{-9} m^2 s^{-1} and decreases by 40% as the concentration of the LiCl solution increases from 0.22 M to 3.97 M (see Table 6). Over the same concentration range, the diffusion coefficient of water in RbCl and CsI shows a slight increase (more apparent in CsI solutions) and finally an overall drop by 33% and 6% respectively at 3.97 M from their values 0.22 M. The decrease in the diffusion coefficient of water with concentration of LiCl can be attributed to fewer unbound water molecules outside the tightly bound hydration sheaths of Li^+ ions and LiCl ion pairs. The initial increase in the diffusion coefficient of water as the salt concentration of RbCl and CsI increases is interesting and may be attributed to the increase in number of water molecules in the more loosely bound hydration cages of these ions. As the concentration increases further increased ion pairing slows down the movement of the ions and water molecules bound to them as discussed above. In CsI solutions, water molecules exist either in ion hydration shells or in pure water clusters; nevertheless, the mobility of water molecules in these two phases does not have a significant difference as discussed previously, therefore the diffusivity of water molecules is relatively independent of the solution concentration.

2.3. Viscosity. The shear viscosity η , which describes resistance to flow, can be calculated by using equilibrium fluctuation of the off-diagonal components of the stress tensor.[51] Averaging over the three off-diagonal components can improve the statistical convergence of the calculation. It was shown by Daivis and Evans[29,51] that, for an isotropic system, the statistical convergence can be further improved by including equilibrium fluctuations of the diagonal components of the stress tensor. The generalized Green−Kubo formula therefore can be expressed as:

$$\eta = \frac{V}{10k_BT}\int_0^\infty \sum_\alpha\sum_\beta q_{\alpha\beta}\langle P_{\alpha\beta}(t)P_{\alpha\beta}(0)\rangle \, dt \quad (9)$$

where V and T are volume and temperature of the simulation cell, k_B is the Boltzmann constant, $q_{\alpha\beta}$ is a weight factor ($q_{\alpha\beta} = 1$ if $\alpha \neq \beta$, $q_{\alpha\beta} = {}^4/_3$ if $\alpha = \beta$), and $P_{\alpha\beta}$ is defined as

$$P_{\alpha\beta} = (\sigma_{\alpha\beta} + \sigma_{\beta a})/2 - \frac{\delta_{\alpha\beta}}{3}(\sum_\gamma \sigma_{\gamma\gamma}) \quad (10)$$

where $\delta_{\alpha\beta}$ is the Kronecker delta ($\delta_{\alpha\beta} = 1$ if $\alpha = \beta$, $\delta_{\alpha\beta} = 0$ if $\alpha \neq \beta$).

By analogy with the Einstein relationship for self-diffusion, the shear viscosity can be calculated by using the mean-square "displacement" of the time integral of the shear components of the stress tensor:[52]

$$\eta = \lim_{t\to\infty}\frac{V}{20k_BTt}\langle\sum_\alpha\sum_\beta q_{\alpha\beta}[L_{\alpha\beta}(t) - L_{\alpha\beta}(0)]^2\rangle = \lim_{t\to\infty}\frac{V}{20k_BTt}\langle\sum_\alpha\sum_\beta q_{\alpha\beta}[\Delta L_{\alpha\beta}(t)]^2\rangle \quad (11)$$

where

TABLE 6: Diffusion Coefficients for Cations, Anions, and Water Shown as a Function of Salt Concentration

concn, M	diffusion coefficient, 10^{-9} m^2 s^{-1}								
	Li^+	Rb^+	Cs^+	Cl^-/LiCl	Cl^-/RbCl	I^-/CsI	H_2O/LiCl	H_2O/RbCl	H_2O/CsI
infinitely dilute solution[17,38]	1.22	1.98	1.88	1.77	1.77	1.60	2.50	2.50	2.50
0.22	1.06	1.86	1.77	1.61	1.52	1.59	2.49	2.54	2.48
0.44	0.99	1.74	1.76	1.47	1.50	1.56	2.49	2.52	2.49
0.90	0.91	1.62	1.64	1.28	1.46	1.48	2.27	2.42	2.57
1.37	0.80	1.52	1.62	1.08	1.39	1.41	2.20	2.35	2.53
1.85	0.75	1.44	1.52	0.97	1.32	1.37	2.07	2.31	2.51
2.36	0.64	1.35	1.42	0.87	1.21	1.28	1.80	2.18	2.50
2.88	0.58	1.25	1.27	0.80	1.10	1.18	1.65	2.12	2.43
3.97	0.43	1.05	1.23	0.62	1.02	1.12	1.44	1.97	2.35

$$\Delta L_{\alpha\beta}(t) = \int_0^t P_{\alpha\beta}(t')\, dt' \quad (12)$$

It has been shown by Mondello and Grest[52] that eqs 11 and 12 give the same results as the Green−Kubo formulation for MD simulations of short-chain alkanes. In this study, we used eqs 11 and 12 to calculate the shear viscosity of the system.

To calculate the shear viscosity more accurately, the correlation was integrated for 20 ps, which is roughly twice the rotational diffusion time of water molecules, and averaged over 40 times the entire equilibrium run.

Shear viscosity for SPC/E water at 300 K was calculated and compared with experimental results to test the simulation procedure. The calculated viscosity of water was around 1.1 g m^{-1} s^{-1} (mPa·s), which is in good agreement with the experimental value of 0.88 g m^{-1} s^{-1} (mPa·s). This indicates that our MD simulations can predict the viscosity of pure water with quite good accuracy. We assume that our calculations of the viscosity of salts in SPC/E water also provide a good representation of the viscosities in real solutions.

The viscosities calculated from our MD simulations of brine solutions as a function of solution concentration are shown in Figure 10. As expected, the size of the ions has a significant influence on the viscosity of the solution. When small ions are present (LiCl solution), the system shear viscosity increases monotonically with solution concentration. As the ion size increases (RbCl solution), the system viscosity shows very weak dependence on the solution concentration. Further increases in ion sizes (CsI solution) leads to an obvious decrease of viscosity as a function of solution concentration. This variation of solution viscosity as a function of ion size and solution concentration has also been observed experimentally by several research groups,[15,53] so our simulations show the same trends.

In LiCl solution, Li^+ ions interact strongly with either water molecules or corresponding anions, and form stable tetrahedral structures, which contribute substantially to a "thicker" system. Though Cl^- ions, due to their large size, do not form strong bonds with water molecules, the influence of cations is dominating. This observation is in good agreement with experimental measurements and theoretical modeling in the literature.[53] Consequently, the mobility of the solution will decrease, and system shear viscosity, which describes mobility macroscopically, will increase. The higher the solution concentration, the more significant role the Li^+ ions play, thus the higher the viscosity. In contrast, when large ions (Cs^+ and I^-) are present in the solution, loose hydrophobic shells are formed around these ions, and the ion/water interaction is not as strong as water/water interaction, accounting for the decrease in the system shear viscosity. In this research, the solution shear viscosity was calculated in a NPT ensemble, which may introduce errors compared to a NVE ensemble. However, the errors are expected to be small with respect to the obvious changes of solution viscosity with solution concentration.

IV. Conclusion

In this study the structure and dynamics of concentrated LiCl, RbCl, and CsI aqueous solutions have been studied successfully by using molecular dynamics simulation. It is found that a small ion such as Li^+, owing to strong electronegativity, significantly immobilizes the water molecules by tetrahedrally bonding with them, and therefore leads to a more compact structure. The higher the salt concentration, the denser the water molecules are packed as indicated by a monotonic increase of water/water coordination numbers as a function of salt concentration. On the other hand, large ions such as Rb^+, Cs^+, and I^- form weak bonds with water molecules, and a loose hydrophobic hydration shell. Thus, the coordination between water molecules decreases with salt concentration. Also, as the ion size increases, the ion/water electrostatic interaction becomes less significant when compared to the hydrogen bonding interaction of water molecules. This agrees satisfactorily with the observed dominating increase of naked Cs^+/I^- ion pair contact, and hydrated Li^+/Cl^- ion pair contact with respect to an increase in salt concentration.

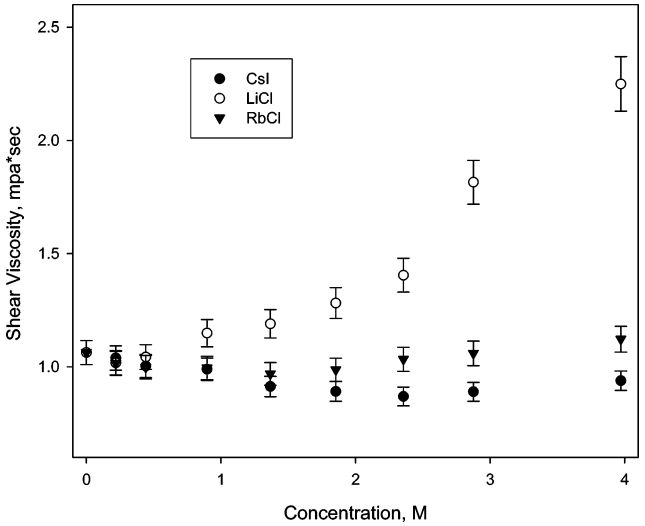

Figure 10. System shear viscosity change as a function of solution concentration.

We have concluded that ion size influences the mobility of water molecules in solution. When small ions such as Li^+ are present, the mobility of water molecules in both the ion hydration shell and the bulk water decreases as a function of salt concentration. In contrast, for solutions containing large ions (CsI and RbCl), the ion/water electrostatic interaction does not contribute significantly to immobilize the water molecules. Consequently, the residence time of water molecules does not show a substantial change with solution concentration. The changes of residence times support the observations of self-diffusion coefficients of particles as a function of salt concentration, which show that when Li^+ ions are present, the diffusion coefficients of water molecules in the solution decrease significantly with salt concentration, and when Cs^+ and I^- ions are present, there is no significant change of the water diffusion coefficients with salt concentration.

The change of system viscosity with solution concentration as determined from MD simulation in this study successfully compliments the experimental results reported in the literature,[17,38] and provides an in-depth understanding regarding the variation of viscosities as a function of ion sizes and salt concentrations from a molecular perspective. For LiCl solutions, the system viscosity increases monotonically with salt concentration due to the strong ion/water interactions in the solution. As the ion size increases, hydrophobic hydration becomes dominating, and leads to negligible variation of system viscosity with salt concentration in the case of RbCl. Further increase in the ion size to Cs^+ and I^- reveals a noticeable decrease of system viscosity as a function of salt concentration. The excellent agreement between the simulation results and the experimental results for the variation of viscosity with ion size and concentration provides information to describe the phenomenological behavior of alkali halide solutions.

Acknowledgment. Financial support provided by the Department of Energy, Basic Science Division (Grant No. DE-FG-03-93ER14315) is gratefully acknowledged. In addition, this study was prompted to some extent by collaborative research supported by NSF under grant Nos. INT-0227583 and INT-0352807. J.C.R acknowledges support from the National Science Foundation under Grant No. CHE 059187.

Supporting Information Available: Plots of radial distribution functions. This material is available free of charge via the Internet at http://pubs.acs.org.

References and Notes

(1) Nickolov, Z. S.; Miller, J. D. *J. Colloid Interface Sci.* **2005**, *287*, 572.
(2) Luck, W. A. P.; Schioeberg, D. *Adv. Mol. Relax. Interact. Processes* **1979**, *14*, 277.
(3) Luck, W. A. P. *Water*: *Compr. Treatise* **1973**, *3*, 211.
(4) Luck, W. A. P. *Proc. Int. Symp. Fresh Water Sea*, *4th* **1973**, *4*, 531.
(5) Max, J.-J.; Chapados, C. *J. Chem. Phys.* **2000**, *113*, 6803.
(6) Max, J.-J.; Chapados, C. *J. Chem. Phys.* **2001**, *115*, 2664.
(7) Max, J.-J.; De Blois, S.; Veilleux, A.; Chapados, C. *Can. J. Chem.* **2001**, *79*, 13.
(8) Terpstra, P.; Combes, D.; Zwick, A. *J. Chem. Phys.* **1990**, *92*, 65.
(9) Dillon, S. R.; Dougherty, R. C. *J. Phys. Chem. A* **2002**, *106*, 7647.
(10) Kaminsky, M. *Z. Phys. Chem.* (*Muenchen, Germany*) **1957**, *12*, 206.
(11) Kaminsky, M. *Z. Naturforsch.* **1957**, *12a*, 424.
(12) Bryant, R. G. *Annu. Rev. Biophys. Biomol. Struct.* **1996**, *25*, 29.
(13) Dang, L. X. *J. Am. Chem. Soc.* **1995**, *117*, 6954.
(14) Dang, L. X. *Book of Abstracts*; 214th ACS National Meeting, Las Vegas, NV, September 7−11, 1997; American Chemical Society: Washington, DC, 1997; PHYS.
(15) Hancer, M.; Celik, M. S.; Miller, J. D. *J. Colloid Interface Sci.* **2001**, *235*, 150.
(16) Lynden-Bell, R. M.; Rasaiah, J. C. *J. Chem. Phys.* **1997**, *107*, 1982.
(17) Koneshan, S.; Rasaiah, J. C.; Lynden-Bell, R. M.; Lee, S. H. *J. Phys. Chem. B* **1998**, *102*, 4193.
(18) Licheri, G.; Piccaluga, G.; Pinna, G. *Chem. Phys. Lett.* **1975**, *35*, 119.
(19) Licheri, G.; Piccaluga, G.; Pinna, G. *Rend. Semin. Fac. Sci. Univ. Cagliari* **1972**, *42*, 85.
(20) Licheri, G.; Piccaluga, G.; Pinna, G. *Gazz. Chim. Ital.* **1972**, *102*, 847.
(21) Lawrence, R. M.; Kruh, R. F. *J. Chem. Phys.* **1967**, *47*, 4758.
(22) Soper, A. K. *J. Phys.*: *Condens. Matter* **1997**, *9*, 2717.
(23) Enderby, J. E.; Cummings, S.; Herdman, G. J.; Neilson, G. W.; Salmon, P. S.; Skipper, N. *J. Phys. Chem.* **1987**, *91*, 5851.
(24) Enderby, J. E. *NATO ASI Ser., Ser. C* **1987**, *205*, 129.
(25) Yamagami, M.; Wakita, H.; Yamaguchi, T. *J. Chem. Phys.* **1995**, *103*, 8174.
(26) Berendsen, H. J. *J. Comput.-Aided Mol. Des.* **1988**, *2*, 217.
(27) Berendsen, H. J. C.; Van Gunsteren, W. F. *NATO ASI Ser., Ser. C* **1984**, *135*, 475.
(28) Dang, L. X. *J. Chem. Phys.* **1992**, *97*, 1614.
(29) Haile, J. M. *Molecular Dynamics Simulation*: *Elementary Methods*; Wiley: New York, 1997.
(30) Uchida, H.; Matsuoka, M. *Fluid Phase Equilib.* **2004**, *219*, 49.
(31) Koneshan, S.; Lynden-Bell, R. M.; Rasaiah, J. C. *J. Am. Chem. Soc.* **1998**, *120*, 12041.
(32) Lee, S. H.; Rasaiah, J. C. *J. Phys. Chem.* **1996**, *100*, 1420.
(33) Lee, S. H.; Rasaiah, J. C. *J. Chem. Phys.* **1994**, *101*, 6964.
(34) Lynden-Bell, R. M.; Rasaiah, J. C. *J. Chem. Phys.* **1996**, *105*, 9266.
(35) Dang, L. X. *Chem. Phys. Lett.* **1992**, *200*, 21.
(36) Dang, L. X.; Smith, D. E. *J. Chem. Phys.* **1993**, *99*, 6950.
(37) Dang, L. X. *Chem. Phys. Lett.* **1994**, *227*, 211.
(38) Dang, L. X.; Smith, D. E. *J. Chem. Phys.* **1995**, *102*, 3483.
(39) Smith, G. D.; Jaffe, R. L.; Partridge, H. *J. Phys. Chem. A* **1997**, *101*, 1705.
(40) Chowdhuri, S.; Chandra, A. *J. Chem. Phys.* **2001**, *115*, 3732.
(41) Chowdhuri, S.; Chandra, A. *J. Chem. Phys.* **2003**, *118*, 9719.
(42) Smith, D. E.; Dang, L. X. *J. Chem. Phys.* **1994**, *100*, 3757.
(43) . Smith, D. E.; Dang, L. X. *Chem. Phys. Lett.* **1994**, *230*, 209.
(44) Dang, L. X. *J. Chem. Phys.* **1992**, *96*, 6970.
(45) Smith, W.; Forester, T. R. *J. Mol. Graphics* **1996**, *14*, 136.
(46) Berendsen, H. J. C.; Grigera, J. R.; Straatsma, T. P. *J. Phys. Chem.* **1987**, *91*, 6269.
(47) Melchionna, S.; Ciccotti, G.; Holian, B. L. *Mol. Phys.* **1993**, *78*, 533.
(48) Impey, R. W.; Madden, P. A.; McDonald, I. R. *J. Phys. Chem.* **1983**, *87*, 5071.
(49) Allen, M. P.; Tildesley, D. J. *Computer Simulation of Liquids*; Oxford University Press: New York, 1987.
(50) Koneshan, S.; Rasaiah, J. C. *J. Chem. Phys.* **2000**, *113*, 8125.
(51) Daivis, P. J.; Travis, K. P.; Todd, B. D. *J. Chem. Phys.* **1996**, *104*, 9651.
(52) Mondello, M.; Grest, G. S. *J. Chem. Phys.* **1997**, *106*, 9327.
(53) Jiang, J.; Sandler, S. I. *Ind. Eng. Chem. Res.* **2003**, *42*, 6267.